RhizoVision Crown: An Integrated Hardware and Software Platform for Root Crown Phenotyping

Anand Seethepalli[1†], Haichao Guo[1†], Xiuwei Liu[1], Marcus Griffiths[1], Hussien Almtarfi[2], Zenglu Li[3], Shuyu Liu[4], Alina Zare[5,6], Felix Fritschi[2], Elison Blancaflor[1], Xuefeng Ma[1], and Larry M. York[1]*

[1] Noble Research Institute, LLC, 2510 Sam Noble Parkway, Ardmore, OK 73401

[2] Plant Science, University of Missouri, Columbia, MO, 65201

[3] Crop and Soil Sciences, University of Georgia, Athens, GA, 30602

[4] Texas A&M AgriLife Research, Texas A&M University, Amarillo, TX, 79106

[5] Computer Science, University of Missouri, Columbia, MO, 65211

[6] Department of Electrical and Computer Engineering, University of Florida, Gainesville, FL, 32601

† Both authors contributed equally to this study.

*Author for Contact.

Email: lmyork@noble.org, Tel: (580) 224-6720

Short title:

Integrated platform for root crown phenotyping

Summary:

The RhizoVision Crown platform integrates cost-effective hardware and easy-to-use software to achieve robust and accurate root crown phenotyping for cereals, legumes, and other crops.

Author contributions:

The RhizoVision Crown platform was conceived by L.M.Y. The software were written by A.S., with contributions to algorithm development from A. Z. The hardware and software had input

from all authors throughout development. H.A. managed the soybean field experiments and root crown phenotyping with F. F. in Missouri using seed from Z. L. Wheat experiments were conducted by X. M., E. B., and X. L. in Oklahoma using seed from S. L., while H.G. organized wheat root crown phenotyping. A.S., H.G., L.M.Y., M. G. and X.L. wrote the manuscript with input from all authors.

Funding sources:

The work was funded by the Noble Research Institute, LLC and the Samuel Roberts Noble Foundation.

ABSTRACT

Root crown phenotyping measures the top portion of crop root systems and can be used for marker-assisted breeding, genetic mapping, and understanding how roots influence soil resource acquisition. Several imaging protocols and image analysis programs exist, but they are not optimized for high-throughput, repeatable, and robust root crown phenotyping. The RhizoVision Crown platform integrates an imaging unit, image capture software, and image analysis software that are optimized for reliable extraction of measurements from large numbers of root crowns. The hardware platform utilizes a back light and a monochrome machine vision camera to capture root crown silhouettes. RhizoVision Imager and RhizoVision Analyzer are free, open-source software that streamline image acquisition and image analysis with intuitive graphical user interfaces. RhizoVision Analyzer was physically calibrated using copper wire and extensively validated with 10,464 ground-truth simulated images of dicot and monocot root systems. The entire platform was further validated by phenotyping 6,256 root crowns from field-grown wheat and soybean populations, and linear discriminant analysis accurately classified the root crowns using the multivariate measurements. Overall, the integrated RhizoVision Crown platform

facilitates state-of-the-art phenotyping of crop root crowns, and sets a standard for which open plant phenotyping platforms broadly can be benchmarked.

INTRODUCTION

Roots serve as the interface between the plant and the complex soil environment with a key function to extract water and nutrients from soils (Lynch, 1995; Meister et al., 2014). Root system architecture (RSA) refers to the shape and spatial arrangement of root systems within the soil, which plays an important role in plant fitness, crop performance, and agricultural productivity (Lynch, 1995; York et al., 2013; Rogers and Benfey, 2015). RSA is shaped by the interactions between genetic and environmental components, and it influences the total volume of soil that roots can explore (Rogers and Benfey, 2015). Many root phenes, or elemental units of phenotype (Serebrovsky, 1925; Lynch, 2011; Pieruschka and Poorter, 2012; York et al., 2013), shape the final root system architecture, including the number, length, growth angle, elongation rate, diameter, and branching of axial and lateral roots (Bishopp and Lynch, 2015). Understanding the contribution of RSA phenes to crop performance is of key importance in food security and for breeding of more productive and resilient varieties in a changing environment.

As roots are hidden underground and require considerable effort to characterize, their research lags behind that of the aboveground parts of the plant (Eshel and Beeckman, 2013), and the genetic and functional basis of RSA remains obscured (Topp et al., 2016). Phenotyping is a major bottleneck in research and a lack of efficient methods for collecting root phenotypic data is limiting progress in using RSA to increase crop productivity (Das et al., 2015; Kuijken et al., 2015). In recent years there has been a shift to image-based phenotyping for enabling relatively high-throughput and accurate measurements of roots. Many of the platforms use 2D imaging with cameras, and involve the use of seedlings on agar plates, germination paper or fabric cloth

in bins (Kuijken et al., 2015). Despite the usefulness of controlling environmental parameters for characterization of root phenotypes, where possible plants should be grown in field conditions as crop growth and development may better represent the agricultural systems in which they are ultimately grown.

Weaver and colleagues (Weaver, 1925; Weaver and Bruner, 1926) pioneered methods for excavating, drawing and photographing root systems, and they have been widely used for over half a century (Böhm, 2012). These classical methods were since modified (Stoeckeler and Kluender, 1938) with the use of water to remove soil particles from the root systems on a large scale, and using high pressure air to penetrate soil pores while leaving roots intact (Kosola et al., 2007). Hydropneumatic root elutriation is a different development by Smucker et al. (1982) to provide a rapid and reproducible approach for separating roots from soils of field soil cores with minimal damage. Traditional excavation methods are most suited for trees and shrubs as the root system of wooden species are generally stronger and more resistant to breaking than the fibrous roots of grasses or annual crops (Böhm, 2012). Other field root phenotyping methods include minirhizotrons and soil coring which both require a large amount of physical labor and time for setting up (Johnson et al., 2001; Böhm, 2012; Wasson et al., 2016). More recently non-destructive root phenotyping methods such as ground penetrating radar and electrical resistance tomography are showing promise, however both techniques are indirect methods for root length and do not provide RSA (Garré et al., 2013; Liu et al., 2018).

Over the past 10 years, root crown phenotyping (York, 2018) has emerged as one of the more common field-based root phenotyping methods, and is characterized by excavation of the top portion of the root system, removal of soil, and measurements, all by whatever means. The definition of root crown in this research is extended from the earlier use of the site where the root

system transitions to the shoot (Beentje, 2010). Root crown phenes such as nodal root number (York et al., 2013; Gao and Lynch, 2016; Slack et al., 2018) and growth angle (Wasson et al., 2012; Trachsel et al., 2013; York et al., 2015; Slack et al., 2018) have been widely reported to correlate with crop above-ground biomass or grain yield performance. The work of Grift et al. (2011) may be the earliest published example of root crown phenotyping in a high-throughput capacity. Root crown phenotyping was widely popularized as “shovelomics” in the work of Trachsel et al. (2011) using visual scoring. While the term “shovelomics” is popular, the extent of its definition are not clear and debate exists whether it only refers to methods based on root crown washing and visual scoring in maize or to other protocols. Therefore, “root crown phenotyping” is proposed as less ambiguous and broadly applicable, as defined above. Root crown phenotyping has been used to enhance the understanding soil resource acquisition by roots of soybean, legume, cowpea, corn and wheat (Trachsel et al., 2010; Colombi et al., 2015; York et al., 2015; York and Lynch, 2015; Burridge et al., 2016; Maccaferri et al., 2016; York et al., 2018).

In order to standardize measurements and increase throughput, image-based phenotyping of crop root crowns has become the standard procedure. The unique steps of image-based phenotyping are acquiring the image and analyzing the image, which are of equal importance with regards to creating a reproducible and reliable protocol. The first example of image-based root crown phenotyping used a custom imaging booth with vision cameras controlled by MatLab and image analysis in MatLab that provided two measures, fractal dimension and top root angle (Grift et al., 2011). The Digital Imaging of Root Traits (DIRT) platform included recommendations for imaging using a DSLR consumer camera that attempted to relax the requirements and focuses on a free cloud-based image analysis pipeline, though a Linux

installation is possible (Bucksch et al., 2014; Das et al., 2015). The Root Estimator for Shovelomics Traits (REST) platform included an imaging 'tent,' DSLR consumer camera controlled using the manufacturer's software, and a MatLab executable requiring the free MatLab runtime for image analysis (Colombi et al., 2015). The Multi-Perspective Imaging Platform (M-PIP) includes five point-and-shoot cameras along a 90 ° arc in an imaging box, command line camera control software for Linux, and MatLab scripts for image analysis (Seethepalli et al., 2018). The cloud-based platform of DIRT requires uploading potentially thousands of root images, which is time consuming, and then downloading the data, and the less-controlled imaging-protocol leads to segmentation failures. The REST platform provides controlled imaging conditions, though not with optimal ergonomics, and the MatLab implementation doesn't include root length. M-PIP requires knowledge of Linux, difficult segmentation of roots form the background using color information, and access to MatLab software. While all these platforms have advanced the field of root crown phenotyping, none are completely optimized for imaging, image analysis, and data processing.

The aim of this study was to develop a phenotyping platform for both high throughput image acquisition and image analysis of root crowns from the field. The imaging hardware is ergonomic for the user, reproducible in any lab, and affordable. The imaging software is the first of its kind optimized for plant phenotyping and usability. The image analysis software is extremely fast, reliable, fully automated, and has a 100% success rate when used with images from the hardware platform. Together, these developments represent an elegant solution for root crown phenotyping, and serve as a benchmark for other plant phenotyping systems.

RESULTS

An integrated hardware and software platform for accelerated phenotyping and knowledge generation

The RhizoVision Crown hardware and software platform represents a state-of-the-art phenotyping solution in root biology, and more broadly a useful benchmark for other phenotyping platforms. The primary focus has been on optimizing the stages of sample loading, recording sample identification, image acquisition, image analysis, and data analysis. A second consideration has been assuring the platform could be used by as many researchers as possible by developing open hardware that can be built by most organizations and free software that is ready-to-run on the widely available Windows operating system with little technical knowledge.

In order to ensure reproducible imaging of crop root crowns that would allow 100% success rates during image analysis, a backlit solution was chosen. An LED flat panel is mounted behind where the root crown is placed and a monochromatic machine vision camera faces the light panel and is focused on the root crown. Root crowns are loaded by attaching to a clip that is affixed to a board. This board fits into an indentation on top of the instrument as to ensure root crowns are loaded into consistent positions and a handle allows the board to be lifted up for replacing the root crown (Fig. 1A). This setup ensures that all images acquired have a white background, with the captured root crown silhouette being primarily black and dark grey (greyscale).

The camera attaches via USB to a laptop computer, and this single cable provides both power and data transfer (Fig. 1C). The RhizoVision Imager software (Fig. 1B) connects to the camera and provides a live view, allows modifying camera settings, saves setting profiles, and acquires images (Seethepalli and York, 2019). Sample identifications (file names) can be typed in for single shots, or a barcode reader can be used for greater throughput and accurate tracking of

sample identity. The barcode setting allows image acquisition to be triggered after a barcode label is scanned and saves the resulting image with the encoded identification. After image acquisition, the root crown is replaced and the process repeated, with throughputs achievable of at least 6 root crowns per minute if previously excavated and cleaned. The dependencies of the Imager software are use of Basler machine vision cameras and installation of the freely available Pylon runtime from the camera manufacturer. All RhizoVision software described are open-source, designed for Windows 10, and do not require installation (just download and run the executable).

Once images are acquired, a separate software named RhizoVision Analyzer (Fig. 2A) is used for batch image analysis (Seethepalli and York, 2019). The user simply provides the directory containing the images, an output directory for generated data, and a greyscale thresholding level for segmenting roots from the background before pressing “Start”. Additional options include saving segmented images and feature images that overlay the features on the segmented image for use in publications and presentations. For the numerical output, pixel units can be converted to physical units if the user supplies the pixels per millimeter. Finally, the diameter ranges for fine, medium, and coarse roots can be defined by the user. The output directory includes a data file with a column for the sample names followed by the 27 extracted measurement columns, and a separate metadata file that stores the user-defined options. The Analyzer software has no additional dependencies to run.

The hardware platform optimizes image acquisition of root crowns to increase throughput and ensure successful image processing. A high level of image quality is achieved with approximately $1,200 USD of hardware that can be assembled by most laboratories, including the aluminum profiles, plastic panels, LED panel, camera, and lens but excluding a laptop

computer. The RhizoVision software are free, open-source, and can be used independently of the imaging box assembly. The Imager software coupled with the imaging box assembly however provides unparalleled ease-of-use in producing reproducible high quality root images that is the first of its kind optimized for plant phenotyping. The Analyzer software can process each image in a fraction of a second on consumer laptop computers and the data output is in a format ready for data analysis pipelines. This integrated platform has transformative potential for root biology and serves as a benchmark for other integrated hardware and software platforms (Lee et al., 2018).

Physical calibration

In order to ensure that the correct physical units were generated by the RhizoVision Analyzer software, copper wires of known diameters ranging from 0.2 – 2.57 mm were scanned with a flatbed scanner at 600 DPI and the correct pixels per mm conversion was supplied to Analyzer. Regression of the computed diameters versus caliper-measured diameters showed nearly exact correspondence ($y = 0 + 1\ x$, $R^2 = 0.99$, $p < .01$) which indicates the physical units provided by Analyzer are accurate when the user supplies the correct pixels to mm conversion (Fig. 3).

Validation using simulated root system images

To validate the diverse measures generated by the Analyzer software, 10,464 simulated images of dicot and monocot root systems from Lobet et al. (2017) were processed (elapsed time 1 hour 7 mins [8-cores, 3.7 Ghz, 16 Gb]). The RhizoVision Analyzer data was correlated with the simulated ground truth data and RIA-J descriptor data (outlined in Lobet et al., 2017). Several root features found in common across the datasets were compared (Fig. 4). The ground truth total root length was under-estimated by Analyzer ($y = -.5 + 1.5\ x$, $R^2 = 0.75$, $p < .01$) (Fig. 4A), which is to be expected as the original simulated roots were three-dimensional but the

processed images are flattened to two dimensions. The descriptor length provided was similar to the Analyzer length ($y = -.1 + 0.97\ x$, $R^2 = 0.99$, $p < .01$) (Fig. 4B), indicating that Analyzer performs similarly to the previously-used software. Tip number ($y = -11 + 1.1\ x$, $R^2 = 0.99$, $p < .01$) (Fig. 4C), root crown area ($y = .2 + 0.96\ x$, $R^2 = 0.98$, $p < .01$) (Fig. 4D), root crown maximum width ($y = -5.1 + 0.99\ x$, $R^2 = 0.99$, $p < .01$) (Fig. 4E), and root crown maximum depth ($y = -5.7 + 1\ x$, $R^2 = 1$, $p < .01$) (Fig. 4F) all indicate that Analyzer extracts phenes that have the same physical units (slopes equal one) and strong correlations with the ground truth and with the phenes extracted from other software.

A tale of two species: comparing root crowns of wheat and soybean

In order to validate the entire hardware and software platform, 3,457 images were acquired of wheat root crowns in Oklahoma and 2,799 of soybean root crowns in Missouri. In Missouri, images were acquired in the field with the imaging system powered by a gasoline generator on the same day the root crowns were excavated. In Oklahoma, images were acquired after wheat root crowns were brought to the lab, stored in a cold room, and imaged within two weeks. In both cases 100% of the root crowns were imaged and successfully processed by the Analyzer software, indicating the hardware provides reproducible images irrespective of plant species that are optimized for image analysis.

For a basic understanding of fundamental differences between the wheat and soybean root crowns, the means and variation were computed (Fig. 5). Definitions of extracted phenes are outlined in Table 1. The total root length of wheat and soybean crowns were 3.1 m and 1.7 m, respectively. The number of root tips was 609 for wheat and 370 for soybean. The maximum widths were 79 mm and 123 mm for wheat and soybean, respectively, while maximum depths were 150 mm and 127 mm for wheat and soybean, respectively. This indicates that wheat has a

deeper and narrower root system, while soybean has a wide but shallow root system. The area of the convex hull surrounding the roots did not differ substantially, indicating the species have roughly the same ability to occupy a soil volume. However, solidity (dividing the root area by the convex hull area) was 0.27 for wheat and 0.21 for soybean, which indicates that wheat may have a greater forage intensively within the soil volume explored. The median root diameters were 0.79 mm and 1.4 mm for wheat and soybean, respectively. Wheat tends to have many more holes (gaps in the root crown) than soybean with 473 and 120, respectively. However, wheat holes are less than half the size of soybean holes on average at 3.4 mm^2 and 7.5 mm^2, respectively. Finally, wheat has a steeper-angled root system compared to soybean based on the average orientation of every pixel in the skeleton, with 49.5° and 42.5° respectively from horizontal, which possibly relates to the greater root crown depth observed in wheat. Together, this data suggests that despite substantial variation within species, these two species are fundamentally different for root crown structure, on average.

While univariate phene comparisons indicated differences between wheat and soybean on average, substantial overlap for all the phenes indicates no single phene can distinguish the two species. Principal component analysis was used to identify the major components of phene combinations that maximize the multivariate variation (Fig. 6). Principal components (PC) 1 and 2 explained 45.2% and 19.5% of the multivariate variation, respectively. The phenes that loaded most strongly onto PC 1 were size-related phenes such as total root length, perimeter, number of root tips, number of holes, several measures of root areas, and some contribution from diameter measures. PC 2 was dominated by width, convex hull area, and measures of root angles, which are indicators of root orientation. Within this 2D space, wheat and soybean were separated but not completely by either axis, but rather along the diagonal of the two components.

To determine the linear combinations that separate the two species, linear discriminant analysis was employed (Fig. 7). Overall classification accuracy from the fitted model was 99.7%, indicating the multivariate data can be used to successfully classify the roots of the two species. The positive loadings onto this single discriminant were dominated by total root length. However, since length could not entirely discriminate independently, it is offset in the linear combination by negative loadings of perimeter, surface area, and network area, and to a lesser extent by the number of holes and coarse diameter frequency. Note that in the descriptive statistics, while means for most of these phenes are different, there is substantial overlap of the standard error and so any one of these phenes are not capable discrimination independently. Therefore, linear combination of multivariate data that maximize the separation of classes is a powerful method to classify root crowns from different species with substantial accuracy.

DISCUSSION

Over the past few years, the throughput, reliability, and standardization of root crown phenotyping has been increased using digital imaging and image-based analysis software such as DIRT (Bucksch et al., 2014), REST (Colombi et al., 2015), and M-PIP (Seethepalli et al., 2018). However, increasing hardware-software integration specifically for root crown phenotyping is promising to further increase of throughput and reliability. Minimizing cost, increasing throughput, and improving reliability are key demands for developing high-throughput root phenotyping platforms. The RhizoVision Crown hardware platform facilitates phenotyping with the end-user in mind by using a backlit approach to capture easily segmented images, a simple clip-and-replace system for exchanging root crowns, and by integration with the RhizoVision Imager software. RhizoVision Imager allows live view so that the user may verify images are high-contrast while framed correctly, stores camera settings, and has a barcode scanning mode

that saves images with the sample identification. The backlit approach and use of imaging software optimized for phenotyping are unique compared all other platforms for root crown phenotyping. The improved quality of images captured enable greater accuracy and precision of root crown phenotyping, and simultaneously broaden the metrics used to characterize roots (Topp et al., 2016). The ergonomics evident in the hardware and control software facilitates high-throughput image acquisition.

Differing from existing root crown phenotyping systems, both RhizoVision Imager and RhizoVision Analyzer are designed to be used by any user on Windows 10. Both provide a graphical interface that is intuitive for new users, can be installed by simply downloading a binary archive to a local directory, and eliminate the need for uploading large files to the cloud before feature extraction like DIRT (Das et al., 2015). RhizoVision Analyzer was physically calibrated, and extensively validated with 10,464 simulated external images of dicot and monocot root systems with no errors. Excellent agreements were observed between root phenes like length, tip number, root crown area, root crown maximum width and root crown maximum depth extracted using Analyzer and published data of the simulated images. Furthermore, the platform was validated with a phenotypic screen of field excavated root crowns for a wheat and soybean population. Root phenes were extracted using the platform and the averages for each species were used to determine fundamental differences between the two species. Linear discriminant analysis using the obtained multivariate data successfully classified the root crowns of the two species with 99.7% accuracy. The wheat and soybean experiments occurred at two different sites with different soils and are meant to be illustrative of the broad applicability of this system, however the data match trends in the literature, such as the shallow foraging nature of first order laterals in soybean or the smaller diameters of wheat roots. In all these image analyses,

no segmentation failures or other errors were discovered. Additional image-based measures could further improve plant classification and characterization of root topology, for example extracting new root phenes such as lateral root branching density, angles and lengths of specific classes of roots through optimized algorithms. Incorporation of morphometric descriptors (Bucksch et al., 2017) could simplify representation of data, such as persistent homology (Li et al., 2018).

In conclusion, the RhizoVision Crown platform is a cost-effective and high-throughput platform that has the potential to democratize access to technologies for root crown phenotyping. The platform builds upon previous platforms (Grift et al., 2011; Bucksch et al., 2014; Colombi et al., 2015; Seethepalli et al., 2018) by optimizing image acquisition using a backlight and the barcode option, using custom imaging software designed for phenotyping, and use of image analysis software with a simple graphical interface designed for batch processing. All software are free and ready-to-use on the most common operating system, Windows 10. The platform has been validated using ground-truth measures of a simulated dataset and successfully extracted root phenes from field-excavated root crowns of cereal and legume species. The ergonomics of use, the integration of all hardware and software, and the extensive validation tests serve as a benchmark for other plant phenotyping platforms. This technology will increase access to root crown phenotyping as a method to acquire data for genetic mapping, use in breeding programs, and understanding how root phenes can address agricultural sustainability and food security.

MATERIALS AND METHODS

RhizoVision Crown Hardware

The RhizoVision Crown hardware platform (Fig. 1A) is a backlit solution designed to produce images in which the background is nearly completely white and the foreground (root

crown) is nearly black because it is a silhouette. This is achieved by use of a 61 cm x 61 cm LED edge lit flat panel light (Anten, 40 watts, 6000K light color) affixed with epoxy to the back of an imaging box. The imaging box is constructed from T-slotted aluminum profiles (80/20 Inc., Columbia City, IN) that were assembled to generate a box measuring 65.5 cm x 65.5 cm x 91.4 cm. Foamed black PVC panels were custom cut (TAP Plastics, Stockton, CA) and placed between profiles to isolate the interior from outside light. A root crown holder was constructed by attaching a spring clap to the bottom of a foamed PVC panel measuring 22.86 cm x 30.48 cm. On the top of the root holder panel a screed door handle was attached for lifting off the instrument. A root crown is clamped onto the holder, and the holder panels is placed in an indentation designed into the top of the imaging box such that root crowns are consistently placed at the desired position. At one end of the imaging box is the LED panel, and on the other is a CMOS sensor monochrome camera (Basler aca3800-um, Graftek Imaging, Inc., Austin, TX). The camera is connected to a laptop computer USB 3.0 port using a USB 3.0 cable (Micro-B male to A male connectors). For the recommended barcode mode, a USB barcode scanner was also connected to the laptop (Tautronics, Fremont, CA). The imaging software is described in the following section.

RhizoVision Imager

The imaging hardware is controlled by RhizoVision Imager (Seethepalli and York, 2019). The software package is open-source with source code located at https://github.com/rootphenomicslab/RhizoVisionImager (for x86_64 processor). The compiled, ready-to-run software binaries can be downloaded at https://zenodo.org/record/2585882 for convenience. The program can connect to multiple Basler USB 3.0 cameras and capture images using the Basler Pylon SDK. For each camera, the parameters Gain, Gamma and Exposure Time

can be changed to suit the experimental needs (Fig. 1B). Using the lenses mounted on the cameras, the aperture and focus of the lens can be modified.

The program starts with a live view for a connected camera. If multiple cameras are connected, the live view for each can be changed in the View menu. The live view can be zoomed in and out to view a specific area in the image. To start capturing images from the connected cameras, a directory location needs to be specified in which to save the images. For single shots, the user may enter an image file name. File names of all the captures images are appended by the camera number and by the number of times the image was taken with the same name the camera number. This ensures that the images are not overwritten.

The program also supports barcode reading for designating filenames and image capture. When a barcode reader is connected to the computer and enabled in Imager, images are captured from all cameras when a barcode is scanned with appended camera number and picture number. The program has a log window, where all the events are logged for review. This includes logging when a new image is captured, camera devices are refreshed or a barcode scanner is attached. The camera settings can be saved as profiles in the program, which may then be reused in later experiments or modified with a text editor. The images can be captured as .BMP, .JPEG, .PNG or .TIFF files. RhizoVision Imager was implemented in C++ and the user interface was developed in Qt, a cross-platform GUI toolkit.

RhizoVision Analyzer

RhizoVision Analzyer is designed to quickly analyze the images acquired using the RhizoVision Crown platform and the Imager software. Analyzer is open-source with source code available at https://github.com/rootphenomicslab/RhizoVisionAnalyzer (for x86_64 processors). The compiled, ready-to-run software binaries can be downloaded at

https://zenodo.org/record/2585892 for convenience. The overall goal in the design of RhizoVision Analyzer was to create a simple-to-use and robust program that batch processes a folder containing root crown images and outputs a data file with the measures for each sample in a form convenient for data analysis. Analyzer has an option to output segmented images as well as processed images on which visual depictions of the extracted features are drawn on the segmented image. Coupled with the optimized image acquisition using the hardware platform, segmentation of the root crown images from the background requires only simple thresholding of the greyscale values for each pixel with minimal loss of data (Fig. 8B). Thresholded (binary) or greyscale images from other platforms may also be used. The input image may have irregular edges which may lead to non-existent skeletal structures being created (Fig. 8C). Hence, the edges of the input image are smoothed so as to remove irregularities along the edge using the Ramer–Douglas–Peucker algorithm (Ramer, 1972; Douglas and Peucker, 1973). After this procedure, overall shape of a root segment does not change substantially, but the skeletal structure now is simpler and has fewer non-existent lateral roots (Fig.8D, Fig. 8F).

On each row of the segmented and smoothed image, each pixel transition from background to foreground (plant root pixel) is counted, obtaining a plant root count profile along the depth of the root crown, from which Median and Maximum Number of Roots are determined (Fig. 9). Maximum Width and Depth are extracted from this smoothed image (Fig. 9C). The Network Area of the image is determined by counting the total number of plant root pixels in the image. Further, a convex polygon is fit on the image and the area of this polygon is noted as Convex Area (Fig. 2C).

A precise distance transform is computed on the line smoothed image in order to identify the medial axis. The distance transform (Felzenszwalb and Huttenlocher, 2012) of an image is the

map of distance of each pixel to the nearest background pixel, here using the Euclidean distance metric (Fig. 9B). The medial axis is a set of loci on the distance transform that are equidistant from at least two background pixels and is identified from the ridges formed on the distance transform map (Fig. 9). In order to make a fully connected skeletal structure, additional pixels are added using the connectivity preserving condition from the Guo-Hall thinning algorithm (Guo and Hall, 1989; Lam et al., 1992) and the endpoints of the ridges are connected using the steepest accent algorithm. The contours of the segmented image are identified for determining the perimeter of the plant root image.

Using the generated skeletal structure, topological properties such as the branch points and end points are identified (Fig. 9B). The skeletal pixels connecting one branch point to another branch or end point are identified as root segments. The number of end points are noted as Number of Root Tips. For each skeletal pixel in every root segment, a 40x40 neighborhood window is selected. All the skeletal pixels on the root segment of the current skeletal pixel are taken within the window and average angle is computed. Using these angles, the numbers of shallow-angled, medium-angled, and steep-roots in an image are noted as histogram bins, by grouping the computed angles in ranges of 0˚ to 30˚, 30˚ to 60˚ and 60˚ to 90˚ respectively. This histogram is normalized and the bins are named as Shallow, Medium and Steep Angle Frequencies. Further, an average of all the angles are computed and noted as Average Root Orientation. A similar normalized histogram is constructed using the skeletal pixels on the root diameter. The histogram bins are allowed for the user to be specified from the user interface of RhizoVision Analyzer. These bins are noted as Fine, Medium and Coarse Diameter Frequency. Also, the Average, Median and Maximum diameters are identified from the diameters of all the skeletal pixels. The plant root area below the pixel having maximum diameter is noted as Lower

Root Area. The segmented and edge smoothed image is color inverted and connected component analysis is performed to count the number of Holes and an average of all the sizes of holes is computed to determine the Average Hole Size. Table 1 briefly describes the list of features extracted from the root crown images.

RhizoVision Analyzer is implemented in C++ using the OpenCV library. The user interface of the program is developed in Qt, a cross-platform GUI toolkit. The program can utilize a CPU's vectorization facilities using Intel's AVX 2.0 technology, to execute the algorithms faster on newer computers. All pixel-based measures are converted to appropriate physical units if the user supplies the number of pixels per millimeter before analysis. Depending on the exact computer system, Analyzer can be expected to routinely process each image in a fraction of a second.

Field Sites and Root Crown Phenotyping

Phenotyping soybeans in Missouri

A soybean recombinant inbred line (RIL) population derived from a cross between PI 398823 and PI567758 was planted at the Bradford Research Center near Columbia, MO on a Mexico silt loam soil (fine, smectitic, mesic Aeric Vertic Epiaqualf). Pre-plant soil tests indicated that no P or K fertilizer application was necessary. Prior to sowing, the seedbed was prepared by one pass with a disc to approximately 0.15 m depth, which was followed by a pass with a harrow. The 185 RILs and the two parental lines were sown in a randomized complete block design with three replications on 14 May 2017 at a density of 344,000 plants ha-1 in 3.04 m long rows with a row spacing of 0.76 m.

Phenotyping wheat in Oklahoma

The wheat population is a recombinant inbred line (RIL) population with 184 F7 lines derived from the cross ‘TAM 112’ x ‘Duster’. The population was created for mapping QTL or genes contributing to a number of important agronomic traits because ‘TAM 112’ is resistant to greenbug and wheat curl mite, and it has superior drought tolerance (Rudd et al., 2014), whereas ‘Duster’ is resistant to Hessian fly and some other diseases (Edwards et al., 2012). ‘TAM 112’ is well adapted to dryland production system in the southern High Plains while ‘Duster’ is one of the most popular wheat cultivars in the southern Great Plains in the past a few years.

Field trials were planted in a randomized complete block design with 3 replications of 1.5 m by 0.9 m plots and seeded at a rate of 148 kg/ha on 11 November 2017 at Burneyville, Oklahoma. The field was clean tilled prior to planting and rain-fed with no supplemental irrigation. For all trials, first fertilization was pre-plant incorporated with 56 kg/ha nitrogen and then top-dressed with 56 kg/ha nitrogen on 23 January 2018 based upon rainfall. Phosphorous and potassium concentrations were sufficient based on soil test results prior to planting. Weeds were controlled with 247 kg/ha of glyphosate at planting and 0.02 kg/ha of Glean XP at Zadoks growth stage 13 at both locations. Post-emergence application of 1.12 kg/ha of 2,4-D was used on 14 February 2018 for broadleaf weed control.

Statistical Analysis

Statistical analyses were employed by the using R version 3.5.1 (R Core Team, 2018) through RStudio version 1.1.45 (RStudio, 2016). Principal component analysis was conducted using the ‘prcomp’ function after scaling and centering the data. The R package ‘MASS’ (Venables and Ripley, 2013) was used for linear discriminant analysis after data was standardized for each measurement such that the mean was zero and the within-group standard deviation was 1 in order to interpret loadings. Accuracy was determined by using jackknifed

(leave one out) predictions, which helps to control overfitting. The R package 'ggplot2' (Wickham, 2016) was used for data visualization and linear regressions were fit using the lm function.

ACKNOWLEDGMENTS

We thank Frank Maulana, Bryce Walker, Wangqi Wang, Tadele Kumssa, Jarron Peoples, Franco Guadarrama, Willie Hart, Matt Hogan, Erika Phillips, Erica Judd for root washing and phenotyping of wheat population.

LITERATURE CITED

Beentje HJ (2010) The Kew plant glossary: an illustrated dictionary of plant terms. Royal Botanic Gardens

Bishopp A, Lynch JP (2015) The hidden half of crop yields. Nat Plants **1:** 15117

Böhm W (2012) Methods of studying root systems, Vol 33. Springer Science & Business Media

Bucksch A, Atta-Boateng A, Azihou AF, Battogtokh D, Baumgartner A, Binder BM, Braybrook SA, Chang C, Coneva V, DeWitt TJ, Fletcher AG, Gehan MA, Diaz-Martinez DH, Hong L, Iyer-Pascuzzi AS, Klein LL, Leiboff S, Li M, Lynch JP, Maizel A, Maloof JN, Markelz RJC, Martinez CC, Miller LA, Mio W, Palubicki W, Poorter H, Pradal C, Price CA, Puttonen E, Reese JB, Rellan-Alvarez R, Spalding EP, Sparks EE, Topp CN, Williams JH, Chitwood DH (2017) Morphological Plant Modeling: Unleashing Geometric and Topological Potential within the Plant Sciences. Frontiers in Plant Science **8:** 900

Bucksch A, Burridge J, York LM, Das A, Nord E, Weitz JS, Lynch JP (2014) Image-based high-throughput field phenotyping of crop roots. Plant Physiol **166:** 470-486

Bucksch A, Burridge J, York LM, Das A, Nord EA, Weitz JS, Lynch JP (2014) Image-based high-throughput field phenotyping of crop roots. Plant Physiology **166:** 470-486

Burridge J, Jochua CN, Bucksch A, Lynch JP (2016) Legume shovelomics: high—throughput phenotyping of common bean (Phaseolus vulgaris L.) and cowpea (Vigna unguiculata subsp, unguiculata) root architecture in the field. Field Crops Research **192:** 21-32

Colombi T, Kirchgessner N, Le Marié CA, York LM, Lynch JP, Hund A (2015) Next generation shovelomics: set up a tent and REST. Plant and Soil **388:** 1-20

Colombi T, Kirchgessner N, Le Marié CA, York LM, Lynch JP, Hund A (2015) Next generation shovelomics: set up a tent and REST. Plant and Soil **388:** 1-20

Das A, Schneider H, Burridge J, Ascanio AK, Wojciechowski T, Topp CN, Lynch JP, Weitz JS, Bucksch A (2015) Digital imaging of root traits (DIRT): a high-throughput computing and collaboration platform for field-based root phenomics. Plant Methods **11:** 51

Douglas DH, Peucker TK (1973) Algorithms for the reduction of the number of points required to represent a digitized line or its caricature. Cartographica: The International Journal for Geographic Information and Geovisualization **10:** 112-122

Edwards JT, Hunger RM, Smith EL, Horn GW, Chen MS, Yan L, Bai G, Bowden RL, Klatt AR, Rayas-Duarte P, Osburn RD, Giles KL, Kolmer JA, Jin Y, Porter DR, Seabourn BW, Bayles MB, Carver BF (2012) 'Duster' Wheat: A Durable, Dual-Purpose Cultivar Adapted to the Southern Great Plains of the USA. Journal of Plant Registrations **6:** 1-12

Eshel A, Beeckman T (2013) Plant roots: the hidden half. CRC press

Felzenszwalb PF, Huttenlocher DP (2012) Distance transforms of sampled functions. Theory of Computing **8:** 415-428

Gao Y, Lynch JP (2016) Reduced crown root number improves water acquisition under water deficit stress in maize (Zea mays L.). J Exp Bot **67:** 4545-4557

Garré S, Coteur I, Wongleecharoen C, Hussain K, Omsunrarn W, Kongkaew T, Hilger T, Diels J, Vanderborght J (2013) Can We Use Electrical Resistivity Tomography to Measure Root Zone Dynamics in Fields with Multiple Crops? Procedia Environmental Sciences **19:** 403-410

Grift TE, Novais J, Bohn M (2011) High-throughput phenotyping technology for maize roots. Biosystems Engineering **110:** 40-48

Guo Z, Hall RW (1989) Parallel thinning with two-subiteration algorithms. Communications of the ACM **32:** 359-373

Johnson M, Tingey D, Phillips D, Storm M (2001) Advancing fine root research with minirhizotrons. Environmental and Experimental Botany **45:** 263-289

Kosola KR, Workmaster BAA, Busse JS, Gilman JH (2007) Sampling damage to tree fine roots: Comparing air excavation and hydropneumatic elutriation. Hortscience **42:** 728-731

Kuijken RC, van Eeuwijk FA, Marcelis LF, Bouwmeester HJ (2015) Root phenotyping: from component trait in the lab to breeding. J Exp Bot **66:** 5389-5401

Lam L, Lee S-W, Suen CY (1992) Thinning methodologies-a comprehensive survey. IEEE Transactions on pattern analysis and machine intelligence **14:** 869-885

Lee U, Chang S, Putra GA, Kim H, Kim DH (2018) An automated, high-throughput plant phenotyping system using machine learning-based plant segmentation and image analysis. PloS one **13:** e0196615

Li M, Frank MH, Coneva V, Mio W, Chitwood DH, Topp CN (2018) The Persistent Homology Mathematical Framework Provides Enhanced Genotype-to-Phenotype Associations for Plant Morphology. Plant Physiology **177:** 1382-1395

Liu X, Dong X, Xue Q, Leskovar DI, Jifon J, Butnor JR, Marek T (2018) Ground penetrating radar (GPR) detects fine roots of agricultural crops in the field. Plant and Soil **423:** 517-531

Lobet G, Koevoets IT, Noll M, Meyer PE, Tocquin P, Pages L, Perilleux C (2017) Using a Structural Root System Model to Evaluate and Improve the Accuracy of Root Image Analysis Pipelines. Front Plant Sci **8:** 447

Lynch J (1995) Root architecture and plant productivity. Plant Physiol **109:** 7

Lynch JP (2011) Root phenes for enhanced soil exploration and phosphorus acquisition: tools for future crops. Plant Physiology **156:** 1041-1049

Maccaferri M, El-Feki W, Nazemi G, Salvi S, Canè MA, Colalongo MC, Stefanelli S, Tuberosa R (2016) Prioritizing quantitative trait loci for root system architecture in tetraploid wheat. Journal of experimental botany **67:** 1161-1178

Meister R, Rajani M, Ruzicka D, Schachtman DP (2014) Challenges of modifying root traits in crops for agriculture. Trends in Plant Science **19:** 779-788

Pieruschka R, Poorter H (2012) Phenotyping plants: genes, phenes and machines. Functional Plant Biology **39:** 813-820

R Core Team (2018) R: a language and environment for statistical computing, R foundation for statistical computing, Vienna, Austria. *In*,

Ramer U (1972) An iterative procedure for the polygonal approximation of plane curves. Computer graphics and image processing **1:** 244-256

Rogers ED, Benfey PN (2015) Regulation of plant root system architecture: implications for crop advancement. Curr Opin Biotechnol **32:** 93-98

RStudio RT (2016) Integrated Development for R. RStudio, Inc., Boston, MA. *In*,

Rudd JC, Devkota RN, Baker JA, Peterson GL, Lazar MD, Bean B, Worrall D, Baughman T, Marshall D, Sutton R, Rooney LW, Nelson LR, Fritz AK, Weng Y, Morgan GD, Seabourn BW (2014) 'TAM 112' Wheat, Resistant to Greenbug and Wheat Curl Mite and Adapted to the Dryland Production System in the Southern High Plains. Journal of Plant Registrations **8:** 291-297

Seethepalli A, York LM (2019) RhizoVision Analyzer: Software for high-throughput measurements from images of crop root crowns *In*. Zenodo. DOI: http://doi.org/10.5281/zenodo.2585892

Seethepalli A, York LM (2019) RhizoVision Imager: Software to control machine vision cameras for plant phenotyping (Version 1.0). . *In*. Zenodo. DOI: http://doi.org/10.5281/zenodo.2585882

Seethepalli A, York LM, Almtarfi H, Fritschi FB, Zare A (2018) A novel multi-perspective imaging platform (M-PIP) for phenotyping soybean root crowns in the field increases throughput and separation ability of genotype root properties. bioRxiv

Serebrovsky AS (1925) "Somatic segregation" in domestic fowl. Journal of Genetics **16:** 33-42

Slack S, York LM, Roghazai Y, Lynch J, Bennett M, Foulkes J (2018) Wheat shovelomics II: Revealing relationships between root crown traits and crop growth. bioRxiv

Smucker AJ, McBurney S, Srivastava A (1982) Quantitative Separation of Roots from Compacted Soil Profiles by the Hydropneumatic Elutriation System 1. Agronomy Journal **74:** 500-503

Stoeckeler J, Kluender W (1938) The hydraulic method of excavating the root systems of plants. Ecology **19:** 355-369

Topp CN, Bray AL, Ellis NA, Liu Z (2016) How can we harness quantitative genetic variation in crop root systems for agricultural improvement? J Integr Plant Biol **58:** 213-225

Trachsel S, Kaeppler S, Brown K, Lynch J (2013) Maize root growth angles become steeper under low N conditions. Field Crops Research **140:** 18-31

Trachsel S, Kaeppler SM, Brown KM, Lynch J (2011) Shovelomics: high throughput phenotyping of maize (Zea mays L.) root architecture in the field. Plant and Soil **341:** 75-87

Trachsel S, Kaeppler SM, Brown KM, Lynch JP (2010) Shovelomics: high throughput phenotyping of maize (Zea mays L.) root architecture in the field. Plant and Soil **341:** 75-87

Venables WN, Ripley BD (2013) Modern applied statistics with S-PLUS. Springer Science & Business Media

Wasson A, Bischof L, Zwart A, Watt M (2016) A portable fluorescence spectroscopy imaging system for automated root phenotyping in soil cores in the field. Journal of Experimental Botany **67:** 1033-1043

Wasson AP, Richards R, Chatrath R, Misra S, Prasad SS, Rebetzke G, Kirkegaard J, Christopher J, Watt M (2012) Traits and selection strategies to improve root systems and water uptake in water-limited wheat crops. Journal of experimental botany **63:** 3485-3498

Weaver JE (1925) Investigations on the root habits of plants. American Journal of Botany **12:** 502-509

Weaver JE, Bruner WE (1926) Root development of field crops.

Wickham H (2016) ggplot2: elegant graphics for data analysis. Springer

York LM (2018) Phenotyping Crop Root Crowns: General Guidance and Specific Protocols for Maize, Wheat, and Soybean. *In* D Ristova, E Barbez, eds, Root Development: Methods and Protocols. Springer, pp 23-32

York LM, Galindo-Castaneda T, Schussler JR, Lynch JP (2015) Evolution of US maize (Zea mays L.) root architectural and anatomical phenes over the past 100 years corresponds to increased tolerance of nitrogen stress. J Exp Bot **66:** 2347-2358

York LM, Lynch JP (2015) Intensive field phenotyping of maize (Zea mays L.) root crowns identifies phenes and phene integration associated with plant growth and nitrogen acquisition. Journal of Experimental Botany **66:** 5493-5505

York LM, Nord E, Lynch J (2013) Integration of root phenes for soil resource acquisition. Frontiers in Plant Science **4:** 355

York LM, Slack S, Bennett MJ, Foulkes MJ (2018) Wheat shovelomics I: A field phenotyping approach for characterising the structure and function of root systems in tillering species. bioRxiv **280875**

FIGURE LEGENDS

Figure 1. RhizoVison Crown hardware and software for root crown imaging. Root crowns are placed into the imaging unit (A) with a backlit panel for framing the root crown and a laptop connected to a vision camera and USB barcode scanner. The vision camera is controlled using the software RhizoVison Imager (C) which has a user interface for controlling camera settings, provides a live camera view, and image export settings.

Figure 2. RhizoVision Analyzer for automated batch analysis of root crown images. (A). The software has a user interface (A) for selecting input and output folders, choosing image threshold levels before analysis, classifying root diameter ranges and saving options. The segmented image (B) and feature image (C) are optionally generated by RhizoVision Analyzer. The feature image shows a blue convex polygon that is fit around the entire root system for extraction of Convex Area. The boundary and skeletal pixels are shown in red and the distance transform is shown in green. The "holes" or the background image patches that were disconnected due to the overlapping of foreground pixels are colored for distinction.

Figure 3. Correlation between diameters of copper wires extracted using RhizoVision Analyzer (RVA) and caliper-measured diameters (each diameter has two points).

Figure 4. Correlations and linear fit equations between root features extracted using Analyzer and ground-truth simulated root data or published descriptors. (A) Scatter plot with fitted linear regression of RVA length against ground-truth data length, (B) Scatter plot with fitted linear

regression of RVA length against original descriptor length, (C) Scatter plot with fitted linear regression of RVA tip number against original descriptor tip number, (D) Scatter plot with fitted linear regression of RVA area against original descriptor area, (E) Scatter plot with fitted linear regression of RVA width against original descriptor width, and (F) Scatter plot with fitted linear regression of RVA depth against original descriptor depth.

Figure 5. Summary of means and standard errors of various features extracted from soybean (n = 2,799) and wheat (n = 3,457) root crown images using the RhizoVision Crown platform.

Figure 6. Principal component analysis of root crown features from the combined wheat and soybean dataset (n = 6,256). Points represent the scores of principal components 1 and 2 (PC1 and PC2) for each species. Labelled lines demonstrate the correlation of feature values to principal component scores.

Figure 7. Linear discriminant analysis indicating the accuracy of classifying as either soybean (scores < 0) or wheat (scores > 0) using the multivariate features generated by the RhizoVision Crown platform.

Figure 8. Example of how RhizoVision Analyzer skeletonizes root crown images before extraction of measurements. A small region of interest is selected (A) and magnified (B) for demonstration purposes. The thresholded image of the region of interest shows that due to the irregular edges, the generated skeletal structure contains lateral roots that are non-existent (shown in blue) (C). The skeletal structure of the root is then smoothed to reduce falsely classified lateral roots before line smoothing operation (D). During the line smoothing operation pixels are either added (shown in red) or deleted (shown in blue). Finally, the skeletal structure of the root after line smoothing operation has the falsely classified lateral roots removed (F).

Figure 9. Example of how RhizoVision Analyzer extracts quantitiative traits from the skeletonized root crown. For each pixel within the root crown skeleton, the corresponding value from the distance map is used to estimate root diameter (A). Topological information is extracted from the skeletal structure such as branch points (shown in blue), root direction change (shown in orange) and end points (shown in green) (B). Finally, for the root counting procedure (C) a pixel transition is marked in a horizontal line scanning operation (shown in blue) for each row and is recorded for counting the number of roots in that row (shown in red).

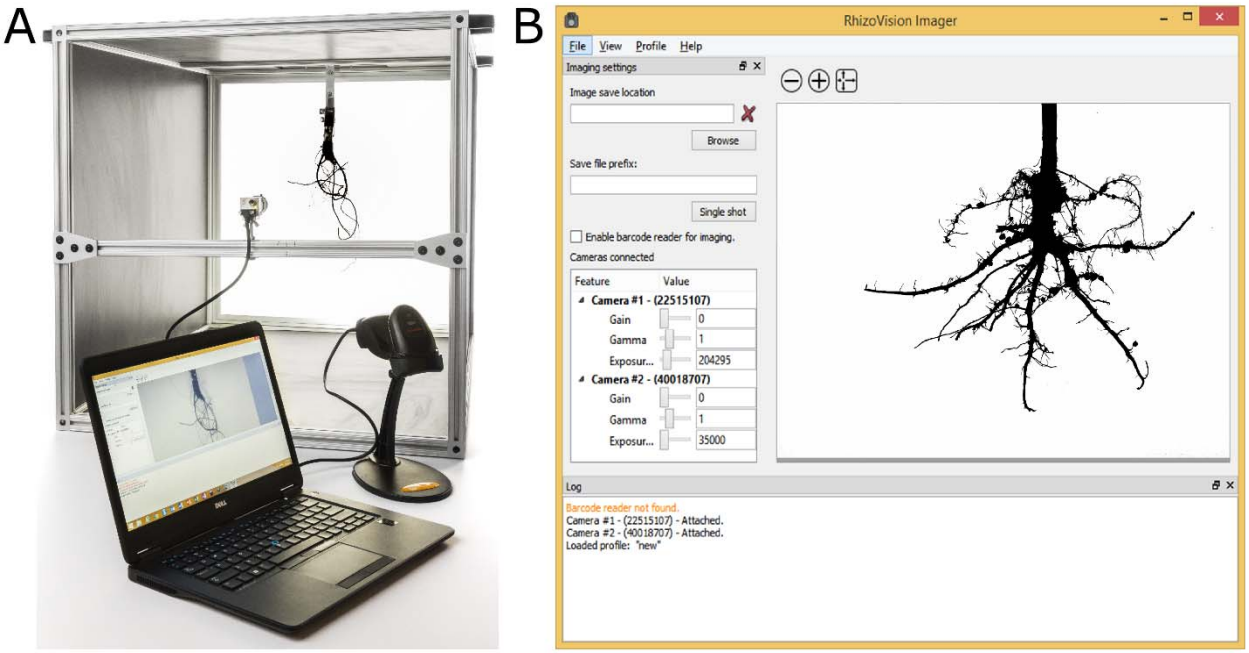

Figure 1. RhizoVison Crown hardware and software for root crown imaging. Root crowns are placed into the imaging unit (A) with a backlit panel for framing the root crown and a laptop connected to a vision camera and USB barcode scanner. The vision camera is controlled using the software RhizoVison Imager (C) which has a user interface for controlling camera settings, provides a live camera view, and image export settings.

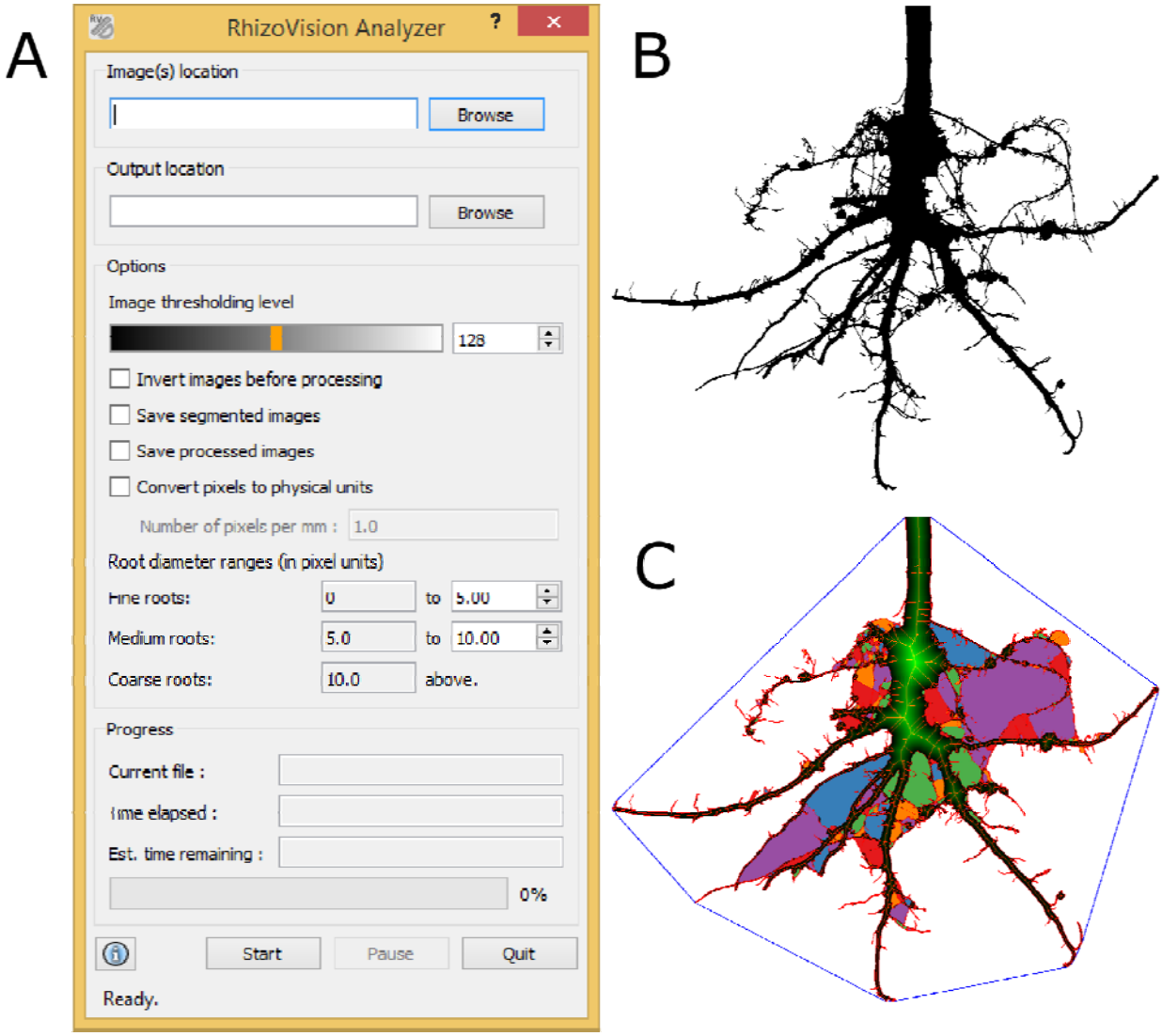

Figure 2. RhizoVision Analyzer for automated batch analysis of root crown images. (A). The software has a user interface (A) for selecting input and output folders, choosing image threshold levels before analysis, classifying root diameter ranges and saving options. The segmented image (B) and feature image (C) are optionally generated by RhizoVision Analyzer. The feature image shows a blue convex polygon that is fit around the entire root system for extraction of Convex Area. The boundary and skeletal pixels are shown in red and the distance transform is shown in green. The "holes" or the background image patches that were disconnected due to the overlapping of foreground pixels are colored for distinction.

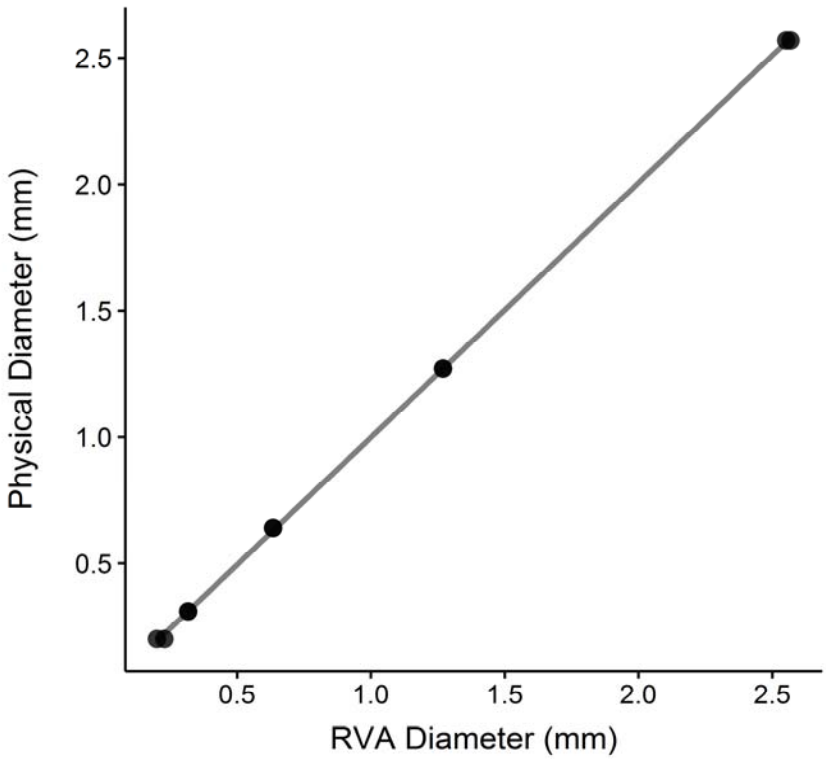

Figure 3. Correlation between diameters of copper wires extracted using RhizoVision Analyzer (RVA) and caliper-measured diameters (each diameter has two points).

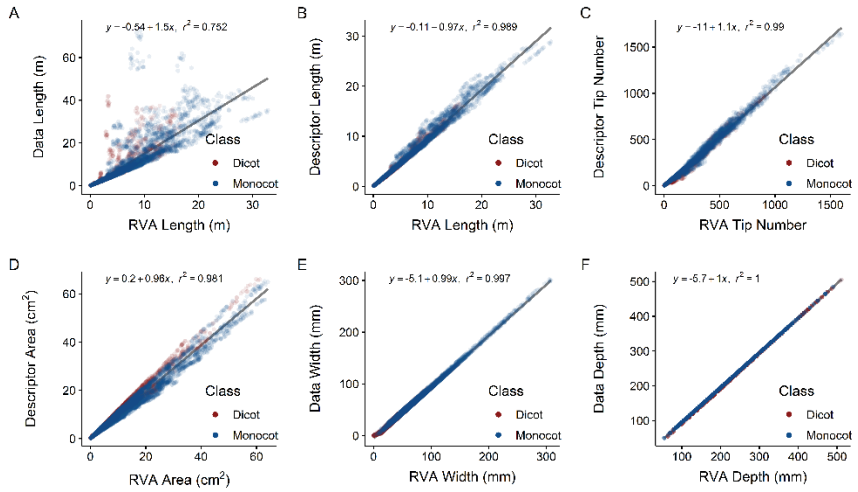

Figure 4. Correlations and linear fit equations between root features extracted using Analyzer and ground-truth simulated root data or published descriptors. (A) Scatter plot with fitted linear regression of RVA length against ground-truth data length, (B) Scatter plot with fitted linear regression of RVA length against original descriptor length, (C) Scatter plot with fitted linear regression of RVA tip number against original descriptor tip number, (D) Scatter plot with fitted linear regression of RVA area against original descriptor area, (E) Scatter plot with fitted linear regression of RVA width against original descriptor width, and (F) Scatter plot with fitted linear regression of RVA depth against original descriptor depth.

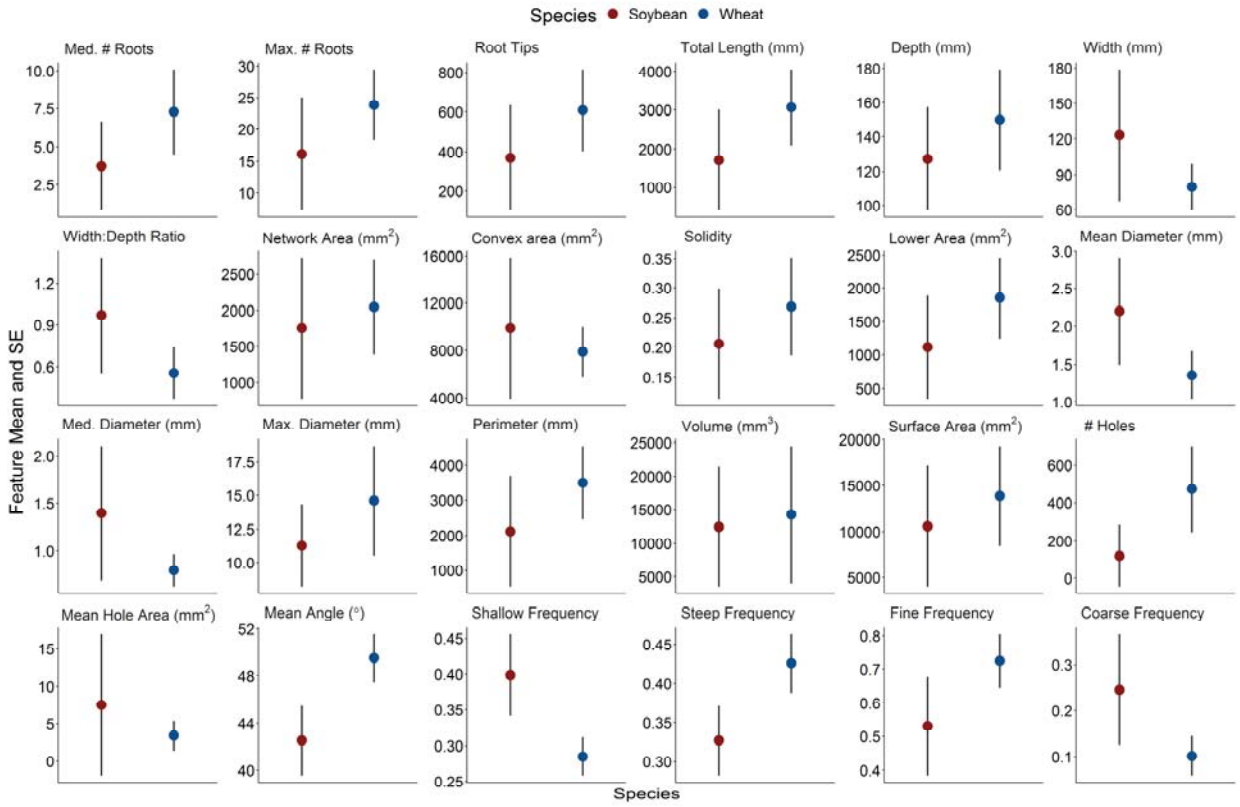

Figure 5. Summary of means and standard errors of various features extracted from soybean (n = 2,799) and wheat (n = 3,457) root crown images using the RhizoVision Crown platform.

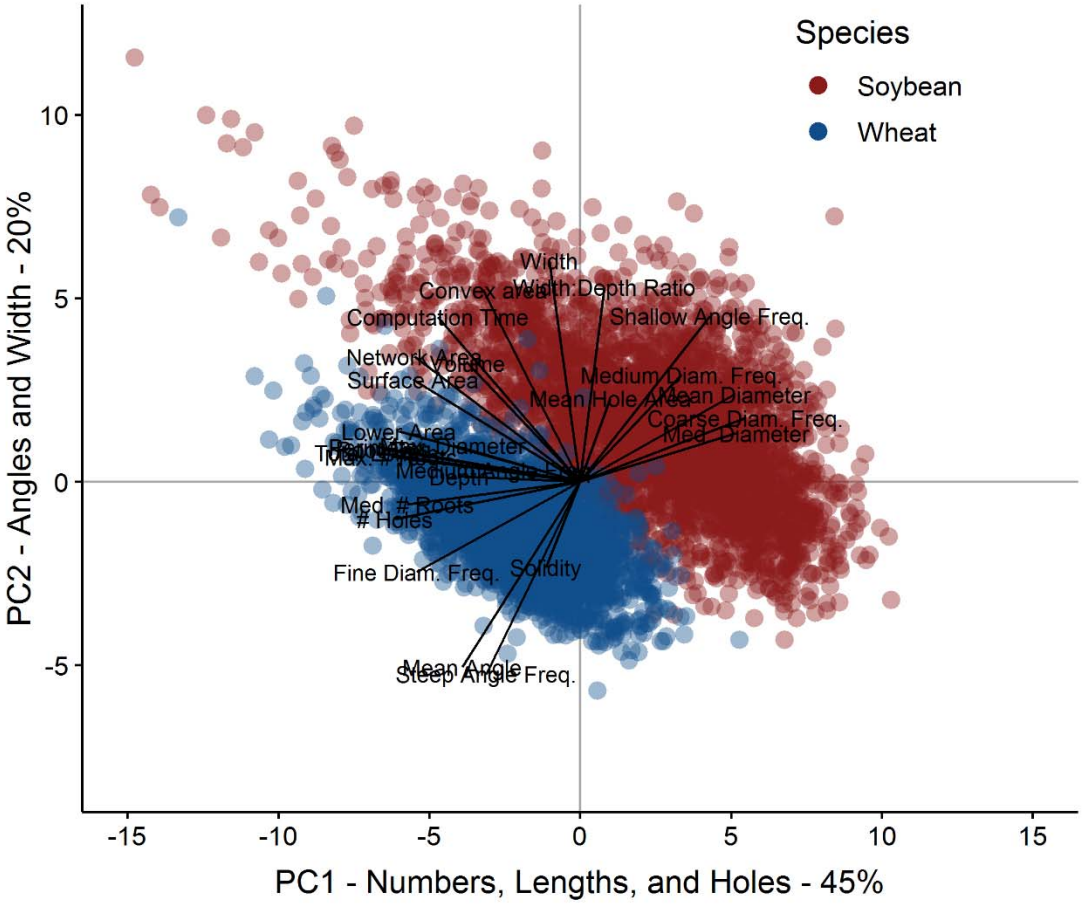

Figure 6. Principal component analysis of root crown features from the combined wheat and soybean dataset (n = 6,256). Points represent the scores of principal components 1 and 2 (PC1 and PC2) for each species. Labelled lines demonstrate the correlation of feature values to principal component scores.

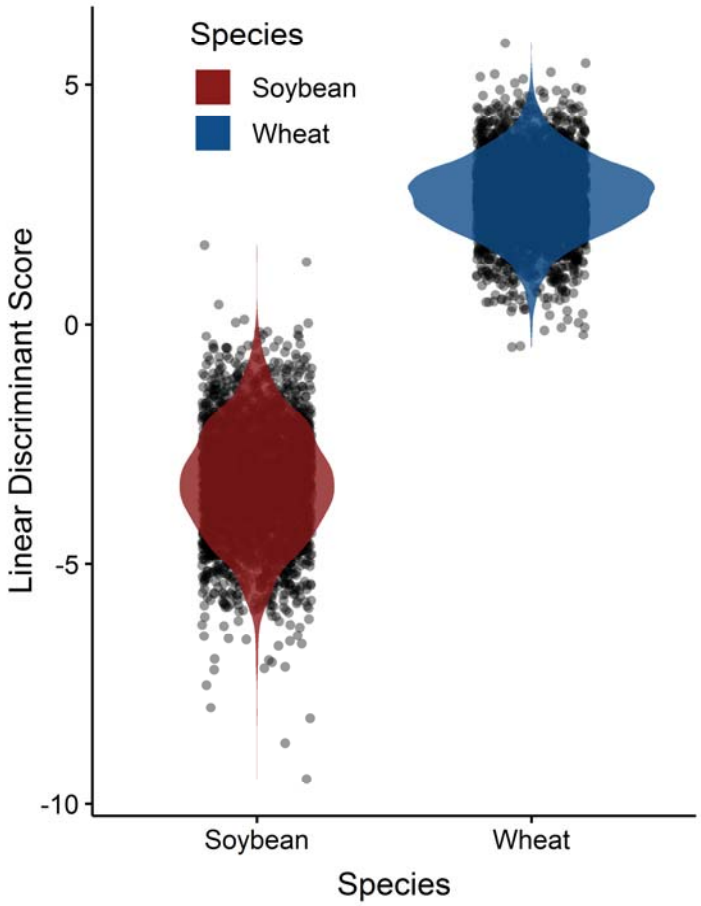

Figure 7. Linear discriminant analysis indicating the accuracy of classifying as either soybean (scores < 0) or wheat (scores > 0) using the multivariate features generated by the RhizoVision Crown platform.

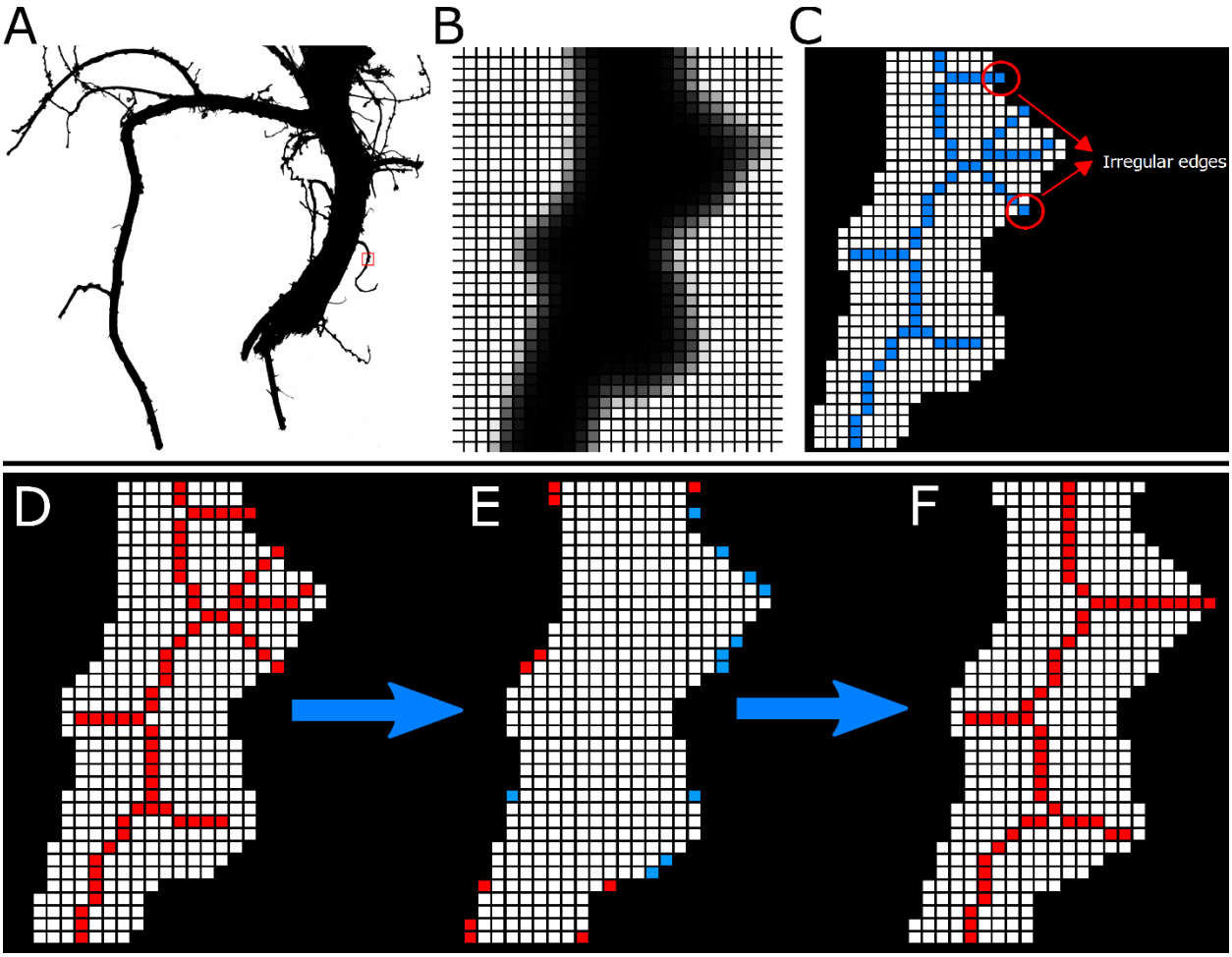

Figure 8. Example of how RhizoVision Analyzer skeletonizes root crown images before extraction of measurements. A small region of interest is selected (A) and magnified (B) for demonstration purposes. The thresholded image of the region of interest shows that due to the irregular edges, the generated skeletal structure contains lateral roots that are non-existent (shown in blue) (C). The skeletal structure of the root is then smoothed to reduce falsely classified lateral roots before line smoothing operation (D). During the line smoothing operation pixels are either added (shown in red) or deleted (shown in blue). Finally, the skeletal structure of the root after line smoothing operation has the falsely classified lateral roots removed (F).

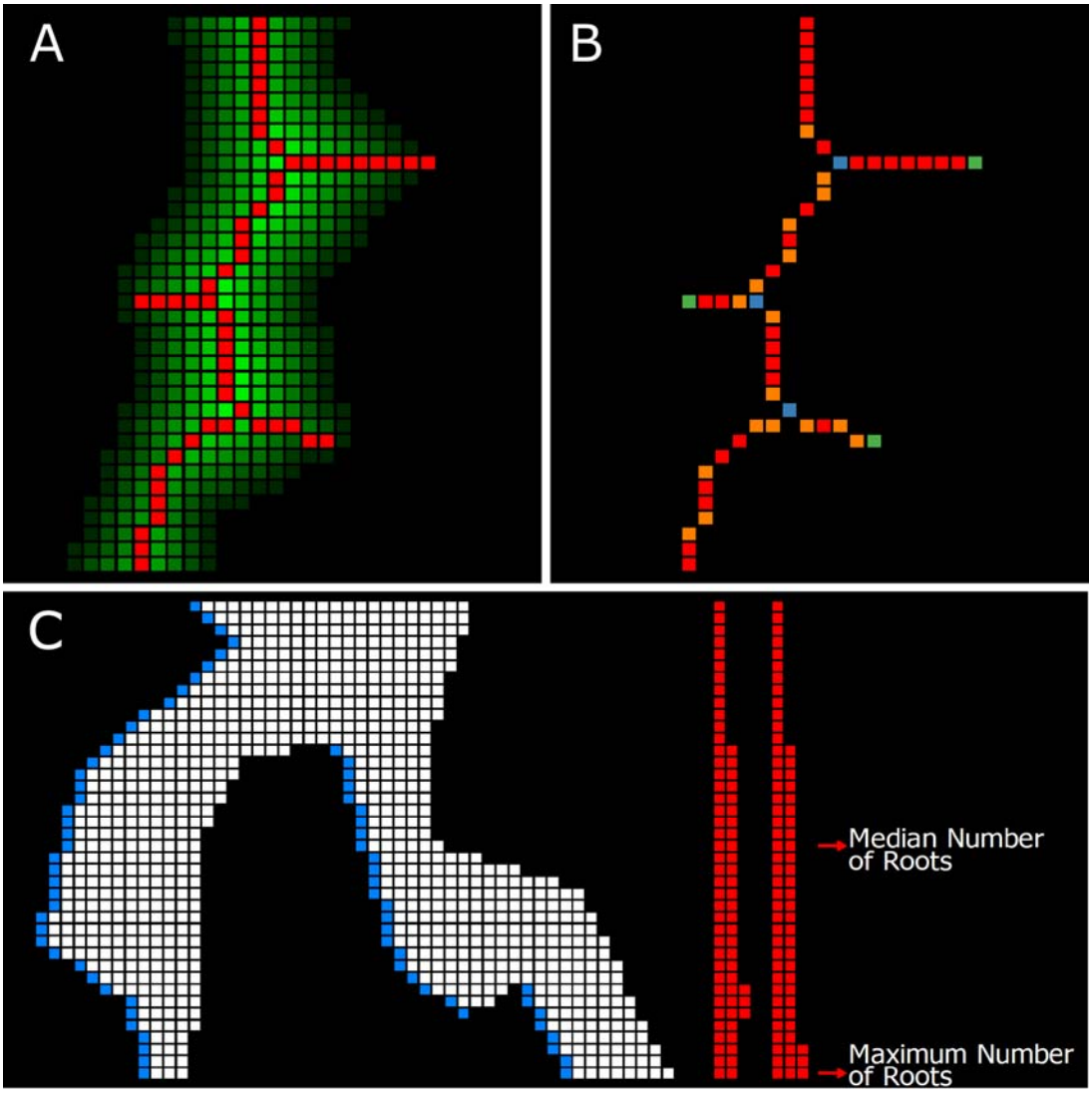

Figure 9. Example of how RhizoVision Analyzer extracts quantitiative traits from the skeletonized root crown. For each pixel within the root crown skeleton, the corresponding value from the distance map is used to estimate root diameter (A). Topological information is extracted from the skeletal structure such as branch points (shown in blue), root direction change (shown in orange) and end points (shown in green) (B). Finally, for the root counting procedure (C) a pixel transition is marked in a horizontal line scanning operation (shown in blue) for each row and is recorded for counting the number of roots in that row (shown in red).

TABLE LEGENDS

Table 1. The list of 27 features extracted from each root crown image by RhizoVision Analyzer.

Features extracted	Description
Median and maximum number of roots	The number of roots are counted by performing horizontal line scans from left to right in each row through the segmented image. In each of the line scan, we check if there is a pixel value transition from the previous pixel value to the current pixel value on its right side. If the current pixel value changes from 0 to 1, we note that a root is present. The number of roots are recorded from each row of the segmented image and the median and maximum number of roots is determined from these values.
Number of Root Tips	Computed by counting total number of tip pixels in the skeletonized image.
Total root length	Computed by counting the total number of pixels in the skeletonized image.
Depth, maximum width and width-to-depth ratio	The trait values for both depth and maximum width of the root in the segmented image. The ratio of maximum width to depth of the image is noted as width-to-depth ratio.
Network area, convex area and solidity	Network area is the total number of pixels in the segmented image. The convex hull of a geometric shape is minimal sized convex polygon that can contain the shape. The ratio of network area and the convex area is noted as the solidity.
Perimeter	Perimeter is the count of total number of pixels in the perimeter image.
Average, median and maximum diameter	For each pixel on the skeletonized image, the distance to the nearest non-root pixel is computed and using this distance as radius a circle is fitted. The diameter of the circle at each pixel is noted as the diameter at that pixel. We get the list of diameters from all the medial axis pixels and determine the average, median and maximum diameter.
Volume and surface area	Using the radii determined earlier, the sum of all cross-sectional areas across all the medial axis pixels are noted as volume and the sum of the perimeter across all the medial axis pixels are noted as surface area.
Lower root area	The lower root area is the area of the segmented image pixels that are located below the location of the medial axis pixel that has the maximum radius.
Holes and Average hole size	Holes are the disconnected background components and indicative of root branching and complexity. They can be counted by inverting the segmented image. The average hole size (area) is also calculated.
Average Root Orientation	For every medial axis pixel, the orientation at the pixel is computed by determining the mean orientation of medial axis pixels in a 40z40 pixel locality. The average of all these orientations is noted as average root orientation.
Fine, Medium, Coarse Diameter Frequencies	From the skeletal image, the medial axis pixels are grouped into fine or coarse roots based on the diameter values at the pixels.
Shallow, Medium, Steep Angle Frequencies	Given the skeletal image, for every pixel in the medial axis, we get the locations of the medial axis pixels in a 40x40 pixel locality and determine the orientation of these pixels in the locality. This orientation is noted for every medial axis pixel. Given these orientations, we calculate the frequency in bins less than 30, less than 60, and less than 90 degrees.
Computational time	The time taken to extract traits for every plant root image.